ANALYSIS OF THE LUNAR SURFACE WITH GLOBAL MINERAL AND MG-NUMBER MAPS. J.T. Cahill[1], P.G. Lucey[1], D. Steutel[1], and J.J. Gillis[1], [1]Hawaii Institute of Geophysics and Planetology, Univ. of Hawaii at Manoa, 1680 East-West Rd. POST 602b, Honolulu, HI 96822 (jcahill@higp.hawaii.edu).

Introduction: Mg-number (Mg#=atomic Mg/(Mg+Fe)) serves as an important petrologic discriminator when analyzing and understanding lunar rocks and crustal evolutionary models. Here we present a new data set of Mg# for the lunar surface that can be used to evaluate crustal materials and modeling in greater spatial and geochemical detail.

The general paradigm for lunar evolution involves formation of a compositionally homogeneous global magma ocean (MO), followed by flotation of cumulate plagioclase crystals that accumulated to form the ferroan anorthositic (FAN) crust between 4.5 to 4.3 Ga [1-3]. After crustal formation, a second stage of magma intrusion and crystallization by Mg-suite rocks occurred during the period of 4.4 to 3.9 Ga [4-6]. However, recent studies of lunar rocks and meteorites suggest that the evolution of the lunar crust may have been more complex than the model briefly described above [7-9]. Studies by [10] and [11] now suggest the possibility of an MO that did not create FAN rocks first. Instead, these authors purpose a MO that crystallized *before* FAN formation. This was then followed by instability in an early mafic cumulate crust, which led to the overturn and eventual rise of FAN rocks via diapirism.

In lunar petrology, Mg# and An (An=atomic Ca/(Ca+Na)) give an approximation of how primitive a rock may be. With important exceptions, lunar rocks with high Mg# and high An are usually geologically older than rocks with more ferroan and more albitic geochemistries. This information in conjunction with mineral data is an invaluable first step towards evaluating lunar crustal rocks. Here, we use Mg# in conjunction with mineral mapping to place lunar surface materials into a new, spatially coherent, lithological, and geochemical context. Future work will also examine the validity of opposing lunar crustal evolution models.

Data: Clementine collected 11 band multispectral data at 100-200 m spatial resolution for most of the lunar surface [12]. The USGS produced a global mosaic sampled at 100-m/pixel for five of these wavelengths from between 400 and 1000 nm [13]. From this mosaic we produced a 1 km resolution mosaic for our analysis. The portion of the data used is for all longitudes, and latitudes between 70 degrees north and south.

Methods: A non-redundant look up table of mineralogy was produced using the minerals olivine, orthopyroxene, clinopyroxene, and plagioclase. These minerals were varied with 5% modal abundance resolution (e.g., 90 pl, 5 cpx, and 5 opx) and constrained to sum to 100%. This yielded 1771 modal mineralogical combinations. Reflectance spectra were then produced between 0.75 and 1.0 μm on the basis of these mineral combinations. The radiative transfer model used to produce these spectra is based upon work by [14-16] and [17]. Input parameters for this model include optical coefficients, modal mineralogy, grain size, and geochemistry (e.g., Mg#). Grain size was held constant at 17 μm and Mg# was varied from 40 to 90 in increments of 5, based upon current spectral understanding of Mg# in mafic minerals from laboratory data. This resulted, in 11 databases of 1771 spectra (i.e., one database for each Mg#).

Both Clementine and the 1771 computed reflectance spectra were normalized by dividing the reflectance by the sum of the four bands used for this model. Each Clementine reflectance spectrum was then compared to each of the 1771 model spectra and an RMS error was taken. The chosen "best-fit" model spectrum for the Clementine pixel exhibited the lowest RMS error. This selection process occurred for each pixel eleven times (for each Mg#), giving 11 best-fit possibilities for each Clementine pixel.

Because Mg# is dependent upon iron, FeO calculations [18] were used as a check for consistency within the model. For example, the difference between Clementine derived FeO [18] and the stoichiometric FeO estimated from our assigned model mineralogy was calculated to yield ΔFeO. For each pixel ΔFeO was calculated for each of the eleven Mg# values. The Mg# chosen for a given Clementine pixel possessed the best agreement between FeO calculation methods (i.e., where ΔFeO=0). We estimate the mean error for these calculations is Mg# ±7.

Results and Discussion: In order to get an idea of the diversity of lunar surface lithologies mapped, minerals were projected onto Stöffler diagrams (e.g., Fig. 1)[19]. Although these diagrams are usually used to classify highlands rocks, for the purpose of this abstract, both highland and mare locals are shown. To first order, the lunar surface shows a wide range of lithologies ranging from pure anorthosites to pyroxene rich norties and pyroxenites. Since the lunar surface consists of both single rock types and well-mixed regolith, these are only considered apparent lithologic classifications until examined further.

Mapping the lunar surface using the geochemical parameter Mg# presents a view of the Moon reminiscent of the spatial distribution of FeO, however, more heterogeneity in regional chemistry is observed (Fig. 2a).

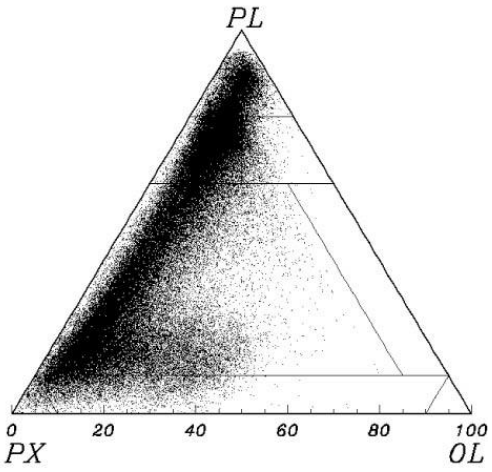

Figure 1a: Pl-Px-Ol diagram of relative lunar surface lithologies.

The statistical distribution of Mg# has a unimodal range of 40-90 (model limits) with a mean of ~75. This Mg# distribution is slightly higher than but consistent with lunar meteorite data (Mg# range 30-80; average 60-70), which is considered to be a random sampling of the lunar surface [9]. A first order observation of mare regions shows an Mg# range of approximately 55-75, while feldspathic highlands locales show a more diverse range of 45-90 (Fig 2a). Several feldspathic highlands regions with Mg# near 90 are also in close proximity to localities where pure anorthosites have been identified by [20]. One such locality is southeast of Grimaldi crater.

Maps of mineralogy, which are a biproduct of selecting ΔFeO, show an abundance of olivine relative to orthopyroxene and clinopyroxene in the farside equatorial region north of South Pole-Aitken basin (SPA) (Fig. 2b). This region is of particular interest because of its location in the Feldspathic Highlands Terrane [21]. Mineral maps also indicate a particularly high abundance of plagioclase in this area relative to other minerals. These data are consistent with regional troctolite and/or troctolitic anorthosite localities identified and studied in detail by [22-23]. This region of high modal olivine and plagioclase also correlates with moderate Mg# (70-75) materials, similar to troctolitic FANs.

Summary: Here we have shown that Mg# can be *quantitatively* determined, mapped, and used in conjunction with mineral data for petrologic study. To a first order, Mg# distribution on the lunar surface is consistent with lunar samples and meteorites. A region of abundant olivine and plagioclase has also been identified on the farside of the Moon north of SPA. This region is further characterized to have an Mg# range of 70-75. Although relative consistency of our analysis with lunar samples has been shown, more in depth analysis of lunar localities and validation of model results with terrestrial and lunar samples in a laboratory setting is necessary.

References: [1] Norman et al. (2003) *MaPS*, 38, 645. [2] Borg et al. (1998) *GCA*, 63, 2679. [3] Alibert et al. (1994) *GCA*, 58, 2921. [4] Nyquist and Shih (1992) *GCA*, 56, 2213. [5] Meyer et al., (1989) LPSC 691. [6] Shih et al. (1993) *GCA*, 57, 915. [7] Bersch et al. (1991) *GRL*, 18, 2085. [8] Floss et al. (1998) *GCA*, 62, 1255. [9] Korotev et al. (2003) *GCA*, 67, 4895. [10] Longhi (2003) *JGR*, 108, 5083. [11] Elkins-Tanton and Parmentier (2004) LPSC #1678. [12] Nozette et al. (1994) *Science*, 266, 1835. [13] Eliason et al., (1999) *LPSC*, #1933. [14] Hapke (1981) *JGR*, 86, 3039. [15] Hapke (2001) *JGR*, 106, 10039. [16] Hapke (1993), New York: Cambridge University Press. [17] Lucey (1998) *JGR*, 103, 1703. [18] Blewett et al. (1997) *JGR*, 102, 16319. [19] Stöffler et al. (1979) *PLPSC*, X, 639. [20] Hawke et al. (2003) *JGR*, 108, 5050 [21] Jolliff et al. (2000) *JGR*, 105, 4197. [22] Tompkins and Pieters (1999) *MaPS*, 34, 25. [23] Lucey (2004) GRL, 31.

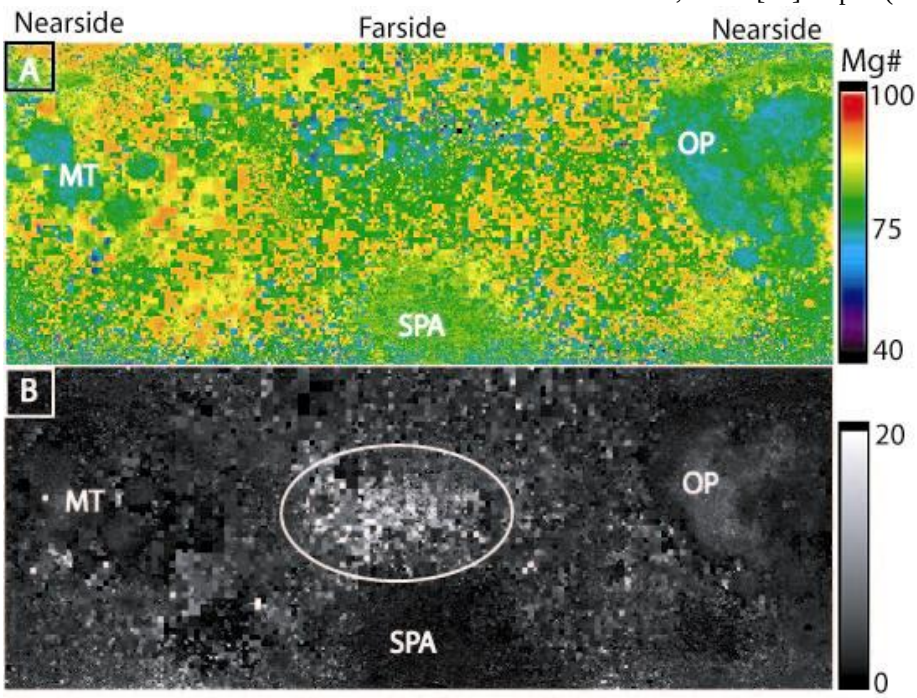

Figure 2ab: A—is a Mg# map of the lunar surface. The color scale is indicated on the right. B- is an olivine concentration map (e.g., ol/(opx + cpx)) of the lunar surface, where the lighter colors indicate a higher concentration. SPA-South Pole-Aitken; OP- Oceanus Procellarum; MT—Mare Tranquillitatis